Physica D 61 (1992) 166–182
North-Holland

PHYSICA D

Gravitational instabilities of thin liquid layers: dynamics of pattern selection

L. Limat, P. Jenffer[1], B. Dagens, E. Touron, M. Fermigier and J.E. Wesfreid
Laboratoire de Physique et de Mécanique des Milieux Hétérogènes, URA CNRS 857, ESPCI, 10 rue Vauquelin, 75231 Paris Cedex 05, France

We present recent results obtained in the study of the instabilities induced by gravity on liquid layers hanging below solid surfaces, in situation of perfect wetting (without contact lines). Two cases are discussed: two-dimensional films of constant volume, and films continuously supplied with "fresh" liquid by an external source. In the first case, we show experimental evidences suggesting that the formation of a two-dimensional structure within the film arises by means of front propagation mechanisms. In the simplest situation, propagation of a one-dimensional structure ("roll" formation), the measured front speed is close to that deduced from the linear marginal stability theory. In the second case, the liquid film is hanging below an horizontal overflowing half-cylinder. Depending on the rate of supply, different regimes are observed (dripping, arrays of parallel jets, triangular sheets). The arrays of drops and jets exhibit interesting spatio-temporal phase dynamics: oscillations, pairing or nucleation of cells, forced tilt waves.

1. Introduction

Gravitational instabilities (or Rayleigh–Taylor instabilities) of thin films [1–5] occur in many practical situations: coating of a solid surface with paint or lubricating agent, formation of aerosols by centrifugal effects [6], boiling of liquids with formation of vapor films [7]. These instabilities also raise fundamental issues regarding the selection of patterns in the non-linear growth regime, and the stability of these patterns with respect to secondary instabilities.

In a recent experiment [4,5], we studied pattern selection in the case of a two-dimensional film first spread by a stabilizing gravity on a solid plate (situation of perfect wetting, the selected fluid being a silicon oil) and then placed in an unstable situation by flipping the plate upside-down. Complex dynamics were observed in this case, different patterns associated to different symmetry orders being formed (see fig. 1): one-dimensional undulations parallel to the boundaries (called lines or "rolls" in analogy with convective instabilities), axisymmetric patterns [5] nucleated by the initial perturbation associated to the presence of dust falling on the interface, axisymmetric patterns breaking in fivefold, sixfold and even sevenfold geometry, hexagonal patterns often obtained by non-linear interactions between the previous ones. After a more or less complicated history, the whole structure evolves towards an hexagonal symmetry. An example of the final array of pendant drops is

[1] Also: Laboratoire de Physique PCEM M2D, Université Paris Sud, Batiment 336, 91405 Orsay, France.

0167-2789/92/$05.00

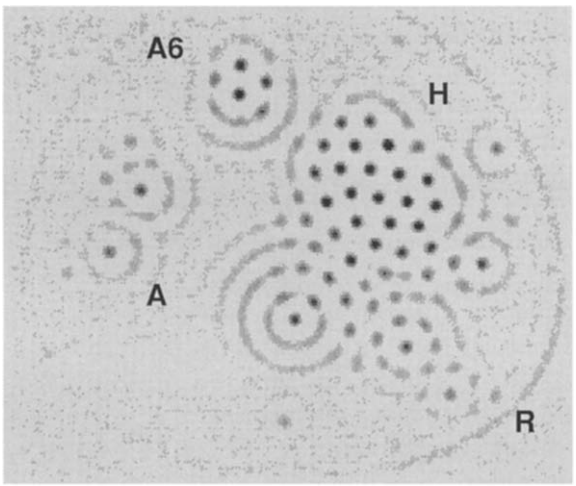

Fig. 1. Two-dimensional patterns observed in the Rayleigh–Taylor instability of a thin layer: "rolls" (R) appearing near the boundary, axisymmetric patterns (A, and A6 breaking into a sixfold symmetry) and hexagonal pattern (H). The thicker regions appear as dark spots, a dye being dissolved in the liquid.

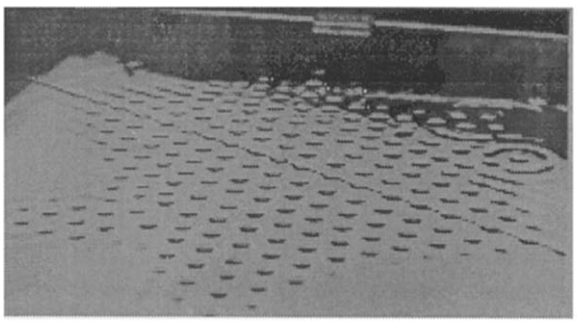

Fig. 2. Array of pendant drops left at the end of the experiment. The drops are seen from above across the solid plate (thick glass).

reproduced in fig. 2. This system of pendant drops exhibits secondary instabilities: depending on their volume and on the existence of defects in the pattern, these drops can fall or remain individually stable. In this last case, the falling of drops occurs by coalescence phenomena, the pairing of two drops leading to a drop big enough to become unstable.

These observations were compared to a theoretical analysis [5,8] built on the lubrication approximation. The essential result was the occurrence of a second order non-linearity in the amplitude equations that favors the coupling of modes separated by angles of 60°. We attributed to this fact the observed tendency to the hexagonal symmetry.

In sections 2.1 and 2.2, we present more recent experiments carried in this geometry. By means of some practical improvements we became able to generate films of nearly uniform and well defined thickness, but with a strong localized thickness gradient near the boundaries, where this thickness must vanish. This initial perturbation gives rise to a very rapid growth of localized rolls near the boundaries. These rolls subsequently break into drops, these drops forming an hexagonal pattern. This structure tends to invade the whole system by successive formation of new rolls, breaking later in new drops. We have studied quantitatively this phenomenon which is seemingly analogous to front propagation into an unstable state [9–12]. These kinds of front propagations are known as mechanisms of pattern selection, the structure left behind the front exhibiting a well defined periodicity that does not coincide with that expected in other conditions (noise amplification for instance). Such fronts occur in various fields including biology [13], hydrodynamic instabilities [14], chemistry [15] and here, perhaps for the first time, in the field of interfacial instabilities. The originality of our system is the possibility to observe two-dimensional aspects in the problem of front propagation. In particular, axisymmetric fronts are also observed, as well as propagation of hexagons on the roll structure.

In section 2.3, we compare the characteristics of these fronts (speed, wavelength left behind) to the predictions of the marginal stability theory discussed by the authors mentioned above, in the linear approximation (known as marginal stability case I). In this approach, one assumes that the dynamics of these fronts is governed by the behavior of the interface in the regions of small amplitude, just ahead of the front. The predictions agree with our observations within the experimental error. This agreement remains however to be discussed, because the non-linear equation governing the interface evolution involves a second-order non-linearity. In this case, non-linear marginal stability (case II) may hold [11], the speed of the front being increased compared to the case I. In addition, our experiment is not perfect (additional large scale thickness gradient, finite size effects, uncertainties in the measurement of thickness and of physical parameters) and remains to be improved.

In section 3 we present a preliminary study of a slightly more complex situation, in which the unstable layer is continuously fed with liquid by an external source. This situation occurs for instance in aerosol generation and film boiling and it is thus important to understand the mechanisms of liquid emissions expected in this case. Depending on the liquid supply flow rate Q, different regimes are observed: at low flow rate, drops are formed on a periodic array, and fall periodically in time. Above a critical value of Q, the array of sites of drop emission is replaced by a periodic array of jets, the liquid emission becoming continuous in time. Above a second threshold, the liquid falls in vertical sheets of triangular shape. Our first observations suggest that the wavelength of the instability in the dripping regime and in the jet regime (spacing between drops and between jets) is roughly independent of the flow rate and very close to that of the Rayleigh–Taylor instability studied in section 2. However, this wavelength is locally perturbed by dynamical processes: coalescence of cells, nucleation of new cells, oscillations of the jet position, compression or dilation waves. We have investigated these phenomena by using a now classical method developed in other one-dimensional systems: by means of a suitable image processing, spatio-temporal (x–t) diagrams are built, allowing us to visualize the evolution of the local periodicity. These spatio-temporal diagrams exhibit rather rich dynamics similar to what is observed on different other systems: printer instability [16], Rayleigh–Bénard instability in thin cells [17], directional solidification of eutectics [18], directional phase transitions in liquid crystal [19], Taylor–Dean instability [20].

We mention two other experiments involving a gravitational instability under continuous supply, but in geometries that are very different from ours. Pritchard [21] studied the instability of the hump left at the end of an inclined plate along which a liquid was flowing. The same regimes of liquid emission (drops, jets and sheets) were observed but Pritchard did not investigate the problems of phase dynamics. More recently Thomé et al. [22] investigated a simple extension of the so-called "printer instability" [16]: in this case the unstable liquid is bounded between two convex vertical cylinders. Our own geometry is closer to the problem of the Rayleigh–Taylor instability of a thin layer discussed in our previous publications [4,5].

2. Front propagations in the Rayleigh–Taylor instability of a thin layer

2.1. Experimental setup

A drop of silicon oil (viscosity $\eta = 480$ cP, density $\rho = 0.973\ \mathrm{g/cm^3}$, surface tension $\gamma = 20.7$ dyne/cm) is spread by gravity on a flat

horizontal glass plate. In order to obtain an homogeneous thickness and well defined boundary conditions, the obtained viscous "pancake" is confined within a hexagonal perimeter which side is equal to 15 cm, drawn on the glass plate with a felt-tip pen for transparencies. This hexagonal shape has been selected in order to reduce the number of topological defects [5]. We have noticed that some particular inks, once dried, alter the wettability of the solid and have the ability to stop oil spreading. After a few days, we obtain a film of nearly uniform thickness ($h_0 = 0.2$–0.3 mm in our experiments) with a strong variation at the boundaries, where this thickness must vanish. The vanishing of the thickness occurs on a scale given by the capillary length $l_c = \sqrt{\gamma/\rho g} = 1.5$ mm.

The glass plate is then turned over in a few seconds (a time much smaller than the typical growth time of instability, of order 300 s [5]), and the development of the instability is recorded by a video camera. A dye is dissolved in the liquid before the experiment, and we record the absorption of the light emitted by a uniform screen placed just below the film (see fig. 3). As seen in fig. 1, thicker regions appear as dark spots, while thinner ones remain lighter. This can be made more quantitative, by using the Beer's law, or by comparing with a sample of liquid contained in a dihedral cell. This method allows us to estimate the local thickness of the liquid with an accuracy of order 0.01 mm. By image processing, it is then possible to reconstruct the thickness profile along a given direction. We mention however that the accuracy given above holds only in weakly deformed regions of the interface: in strongly deformed regions, the curvature may also become another source of light modulation.

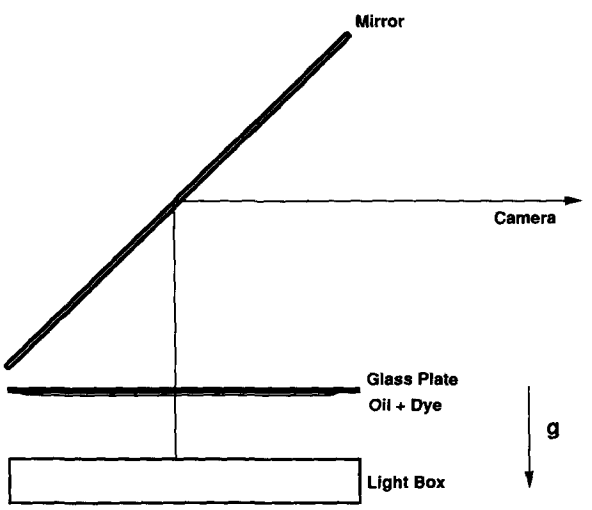

Fig. 3. Schematic experimental set up used in the study of two-dimensional films.

2.2. *Front propagation phenomena: qualitative observations*

A typical sequence of observations is reproduced in fig. 4. Initially, a system of lines ("rolls") is nucleated near the boundaries and progressively invades the surface of the liquid. Near the corners of the hexagons, where two boundaries cross each other, the interference of the two sets of lines gives rise to the nucleation of a hexagonal pattern. In turn, this hexagonal structure invades the roll system. We then observe two kinds of fronts: a front separating the rolls from the regions of unperturbed thickness (formation front of the rolls), and a roll–hexagon front. At first, the transition roll–hexagons involves the breakup of the first roll into drops, this phenomenon involving again a front propagation along this roll (see first picture in fig. 4). This process is repeated for the second rolls and so on. At a later stage it becomes more difficult to distinguish between this "longitudinal" propagation mechanism and a possible "transverse" one.

In general the domains occupied by the "rolls"

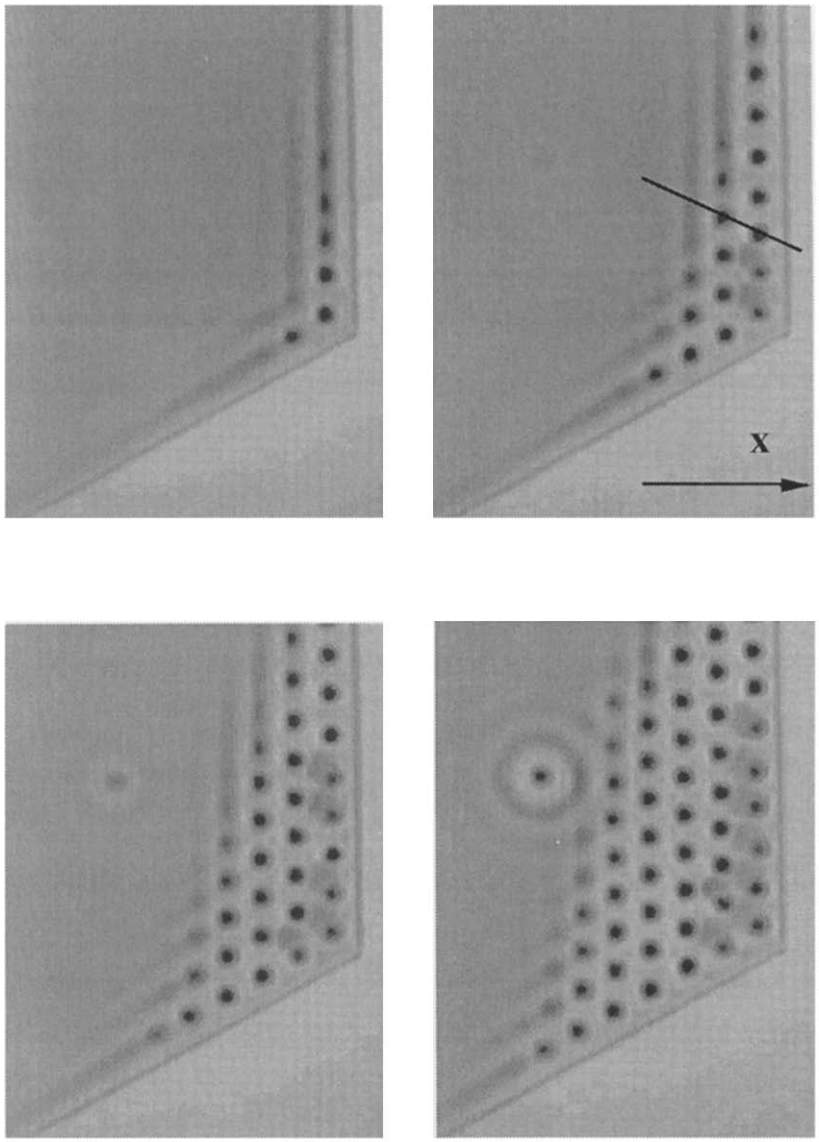

Fig. 4. Time evolution of the instability observed on a film with hexagonal boundaries. The time interval between two pictures is 90 s.

are rather narrow, and the number of rolls visible ahead of the hexagonal structure remains of order two. In these conditions, the sequence of events reproduced in fig. 4 can also be understood as the propagation of the hexagonal structure into regions of unperturbed thickness, the front exhibiting a substructure involving these two rolls.

We extract from the pictures of fig. 4 the thickness profiles along one of the main direc-

tions of the hexagonal structure at different times separated by a constant time interval. These profiles are reproduced in fig. 5 and suggest a front propagation at constant speed. As it appears in fig. 4, the front speed is not uniform throughout the sample. We think that a large scale thickness gradient is responsible for this effect (the typical time-scale is proportional to the cube of the local thickness [1–5]). In fig. 4, the thickness is maximum in the corner of the sample, the horizontally and flatness of the glass plate being not perfect. More accurate experiments are now under way.

Another kind of front propagation is visible in fig. 4. In addition to the pattern nucleated by the boundaries, an axisymmetric one is also growing around a speck of dust. This dust induces an initial perturbation of the interface analogous to that associated to the boundaries although of presumably smaller amplitude. A process of invasion of the liquid surface by this pattern very similar to that of the rolls also occurs, successive annuli being formed as time increases.

From the data of fig. 5, we deduce a typical value of the speed of front propagation. This

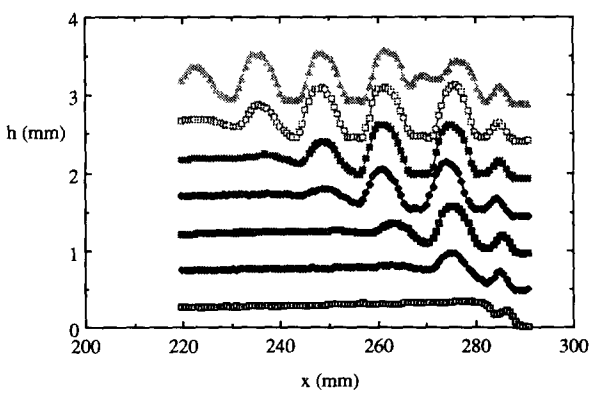

Fig. 5. Time evolution of the thickness profile recorded along the line drawn on fig. 4. The profiles have been shifted for clarity and are separated by a time interval of 30 s (x designates the coordinate in the direction perpendicular to the rolls).

speed is found of order $v^* \approx 0.18 \pm 0.03$ mm/s in the studied region, where the initial thickness is bounded between 0.24 and 0.3 mm. As mentioned above, this speed is presumably proportional to the cube of the initial thickness. We also estimate the wavelength of the pattern left behind the front: $\lambda_L = 1.25 \pm 0.05$ cm (averaged on four periods in the hexagonal state). At the accuracy of our measurements, this value cannot be distinguished from that associated to the most unstable mode in the linear approximation $\lambda_M = 2\pi\sqrt{2}\sqrt{\gamma/\rho g} = 2\pi\sqrt{2}\, l_c \approx 1.3$ cm.

2.3. *Formation front of the rolls: a theoretical attempt*

We determine now the front propagation velocity and the wavelength selected by this process using the theory of marginal stability [9–12] and compare these predictions with our experimental results. In the lubrication approximation, the evolution equation of the local thickness $h(x, y, t) = h_0 + \zeta(x, y, t)$ is given by [1,3,5]

$$\frac{\partial \zeta}{\partial t} + \frac{1}{3\eta}\nabla\cdot[(h_0+\zeta)^3\nabla(\rho g\zeta + \gamma\nabla^2\zeta)] = 0\,. \quad (1)$$

This equation results from mass conservation, in which the horizontal flow rate is proportional to the local pressure gradient in the horizontal direction $\nabla P = \nabla(\rho g\zeta + \gamma\nabla^2\zeta)$. The "mobility" of the liquid is proportional to the cube of the local thickness $(h_0 + \zeta)^3$ because of the structure of the flow in the vertical direction. In the lubrication approximation, the velocity profile is parabolic, the viscous shear stress vanishing at the free surface. In the linear approximation, eq. (1) yields the following dispersion relationship for Fourier modes $\zeta = \zeta_0 \exp(iqx + \sigma t)$:

$$\sigma = \frac{h_0^3}{3\eta}(\rho g q^2 - \gamma q^4)\,. \quad (2)$$

As mentioned above, the wave-number associ-

ated to the "most unstable" mode is given by $q_M = \sqrt{\rho g/2\gamma}$ (wavelength $\lambda_M = 2\pi/q_M = 2\pi\sqrt{2}\, l_c$) and the corresponding growth rate is equal to $\sigma_M = h_0^3 \rho^2 g^2/12\eta\gamma$.

We consider the simplest case of a formation front of the lines ("rolls"), assumed to be parallel to the nucleated lines. In addition, we admit that the properties of the front are selected by mechanisms of linear marginal stability (case I), as discussed by Dee and Langer [9]. In this case, these properties are selected in the region just ahead of the front, where ζ is very small and can be assumed to vary as $\zeta \approx \exp[iq^* x + \sigma(q^*)t]$. The wave-number q^* is complex, the imaginary part taking into account the amplitude modulation. It can be deduced together with the speed of the front v^* by the conditions [9]

$$iv^* + \frac{d\sigma}{dq} = 0\,, \quad \mathrm{Re}(iv^* q + \sigma) = 0\,. \tag{3}$$

The wave-number of the pattern left behind the front q_L is obtained by writing a condition of conservation of the number of rolls as seen by two observers moving at a speed v^*, the first one ahead of the front, and the second one behind the front: $q_L v^* = v^* \,\mathrm{Re}\, q^* + \mathrm{Im}\, \sigma(q^*)$. These equations give

$$v^* = 4.59 q_M \sigma_M = 0.54 \frac{h_0^3 (\rho g)^{3/2}}{\eta \gamma^{1/2}}\,, \tag{4a}$$

$$q_L = 1.08\, q_M = 1.48\sqrt{\rho g/\gamma}\,. \tag{4b}$$

We have measured in separate experiments the physical properties of the silicone oil: $\gamma = 20.7 \pm 0.2$ dyne/cm (ring tensiometer), $\eta = 480 \pm 10$ cP (low shear Couette rheometer), $\rho = 0.973 \pm 0.005$ g/cm^3 (picnometer). As mentioned above, the propagation of the front has been studied in a region of initial thickness $h_0 = 0.27 \pm 0.03$ mm. These values lead to a theoretical estimate of v^* of order $v^* = 0.14 \pm 0.05$ mm/s. This value is in agreement with the measured one $v^* \approx 0.18 \pm 0.03$ mm/s. As mentioned above, our wave-length measurements are not accurate enough to distinguish between λ_L and λ_M. However, repeated experiments suggests that the ratio of these two quantities λ_M/λ_M is slightly smaller than 1 (of order 0.95) in agreement with (4b).

In summary, our results are roughly consistent with the theory of linear marginal stability (case I) of the front. However, the following points must be taken into account:

– In our experiment, the front is not parallel to the rolls, because of an additional large scale thickness gradient. The measured velocity is in fact the component of v^* perpendicular to the rolls.

– Usually, the predictions of the theory of marginal stability of the fronts hold asymptotically, when a large enough number of cells have been created by the front propagation process. In our experiment, it is difficult to observe a "free propagation" on more than five periods (as in fig. 5), the pattern nucleated by the boundaries interfering with those nucleated around uncontrolled dusts. In these transient conditions, the measured speed is expected to be smaller than the asymptotical one.

– Another problem comes from the non-linearities involved in the evolution equation. After rescaling eq. (1) by replacing the quantities ζ, x, y, t by dimensionless equivalents ζ/h_0, $q_M x$, $q_M y$, $\sigma_M t$, and after separating linear and non-linear contributions, one gets

$$\frac{\partial \zeta}{dt} + 2\nabla^2\zeta + \nabla^4\zeta + 3\nabla\cdot[\zeta\nabla(2\zeta + \nabla^2\zeta)] + 3\nabla\cdot[\zeta^2\nabla(2\zeta + \nabla^2\zeta)] + \nabla\cdot[\zeta^3\nabla(2\zeta + \nabla^2\zeta)] = 0\,. \tag{5}$$

This equation contains a second order non-linearity. It is known in this case that the linear theory of marginal stability (case I), may not hold [11]. In summary, the properties of the

front are not selected in the regions of small ζ, and a non-linear marginal stability approach mush be used (case II). Van Saarloos [11] has shown that, in the case of the generalized Swif–Hohenberg equation

$$\frac{\partial \zeta}{\partial t} = [\varepsilon - (1 + \partial x^2)^2]\zeta + b\zeta^2 - \zeta^3 , \qquad (6)$$

the expected velocity becomes larger than the value deduced from the linear approach, the discrepancy increasing with the weight b of the second order non-linearity. The linear part of eq. (5) coincides with that of the Swift–Hohenberg equation when the control parameter ε is set to the value $\varepsilon = 1$. We thus suggest that our system could belong to case II of marginal stability, v^* being in fact larger than the value 4.59 obtained in the linear approximation. More accurate measurements of v^* are under way.

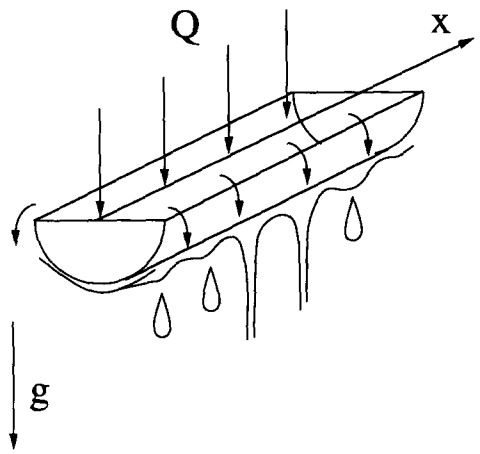

Fig. 6. Geometry of the experiment carried on a one-dimensional film under continuous supply. A hollow half-cylinder, uniformly supplied with liquid, overflows, the instability occurring at the lowest generating line.

3. Films under continuous supply: a one-dimensional experiment

3.1. Experiment – general observations

As sketched in fig. 6, an horizontal, hollow half-cylinder is supplied with liquid at a constant rate. The liquid overflows, runs over the external sides and is gathered below the cylinder. The resulting layer is in an unstable situation with respect to gravity, and breaks into drops or jets depending on the flow rate Q. We use a plexyglass cylinder of length $L = 25$ cm, the internal and external radii being equal to $R_1 = 2$ cm and $R_2 = 2.5$ cm. The liquid is again a silicone oil (density $\rho = 0.97\ \mathrm{g/cm^3}$, surface tension $\gamma = 21$ dyne/cm) that perfectly wets the cylinder and avoids formation of contact lines. Most of our results have been obtained with a viscosity equal to $\eta = 20$ cP, but we have also performed some preliminary experiments with a smaller value: $\eta = 2$ cP. It is to be noted that the external radius of the cylinder (2.5 cm) is large compared to the capillary length $l_c = \sqrt{\gamma/\rho g} \approx 1.5$ mm. This should avoid a possible coupling of the gravitational instability with the Rayleigh instability of a cylindrical fluid film studied by Hammond [23].

Depending on the flow rate, different regimes of liquid elimination are observed. At low flow rate, drops are formed and fall periodically in time (fig. 7), the sites of drop emission being ordered on a periodic array along the cylinder. As for drops formed at an orifice [24], all the liquid gathered in a drop does not fall, and a residual drop remains after the fall. In turn, this drop begins to grow until a new fall occurs, when a critical size is reached. At larger rates, a different structure is observed, consisting of an ordered array of vertical jets (fig. 7). Upon a further increase of the flow rate, the array of jets is finally replaced by liquid sheets of triangular shape. In the transition domains, mixed states (drops and jets, or jets and sheets) are also obtained.

We focus our study on the dripping regime and

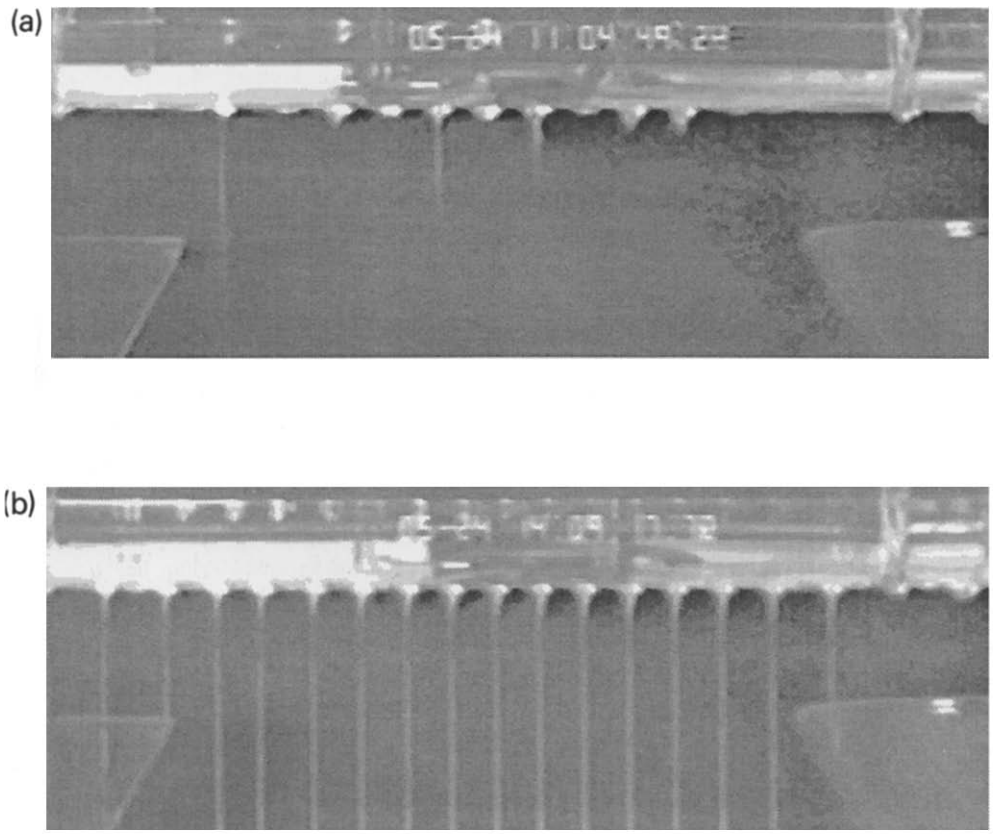

Fig. 7. (a) Array of drop emission sites observed in the "dripping" regime, and (b) array of jets observed in the "jet" regime. The width of the recorded field is equal to 24 cm.

on the jet regime. In the case $\eta = 20$ cP, the transition between these two regimes is found to occur for a critical value of the flow rate $Q_c \approx 2.5\ \mathrm{cm}^3/\mathrm{s}$. Near this transition, jets and drops coexist in the range $2 < Q < 3\ \mathrm{cm}^3/\mathrm{s}$, the number of jets being a function of Q with hysteresis. A similar phenomenon is observed in the case $\eta = 2$ cP, the critical flow rate being of order $Q_c \approx 3\ \mathrm{cm}^3/\mathrm{s}$, the mixed regime covering the domain $2 < Q < 4\ \mathrm{cm}^3/\mathrm{s}$. Following Pritchard [21], one can define a Reynolds number $\mathrm{Re} = Q/L\nu$ built on the flow rate Q, the length of the system in the x direction L, and the kinematic viscosity $\nu = \eta/\rho$. This allows to compare our observations with Pritchard's ones. In the case $\eta = 22$ cP, our transition drop-jet region is given by $0.11 < \mathrm{Re} < 0.15$, values very similar to those deduced from Pritchard's pictures obtained with oil with viscosity $\eta = 80$ cP: $0.13 < \mathrm{Re} < 0.2$. However, our experiments carried for a lower viscosity $\eta = 2$ cP leads to values ten times smaller. This suggests that other non-dimensional parameters must be taken into account in the description of the flow.

In all our experiments, the arrays of sites where dripping takes place, as well as the array of jets are regular periodic structures, with local perturbations of the wavelength that we will

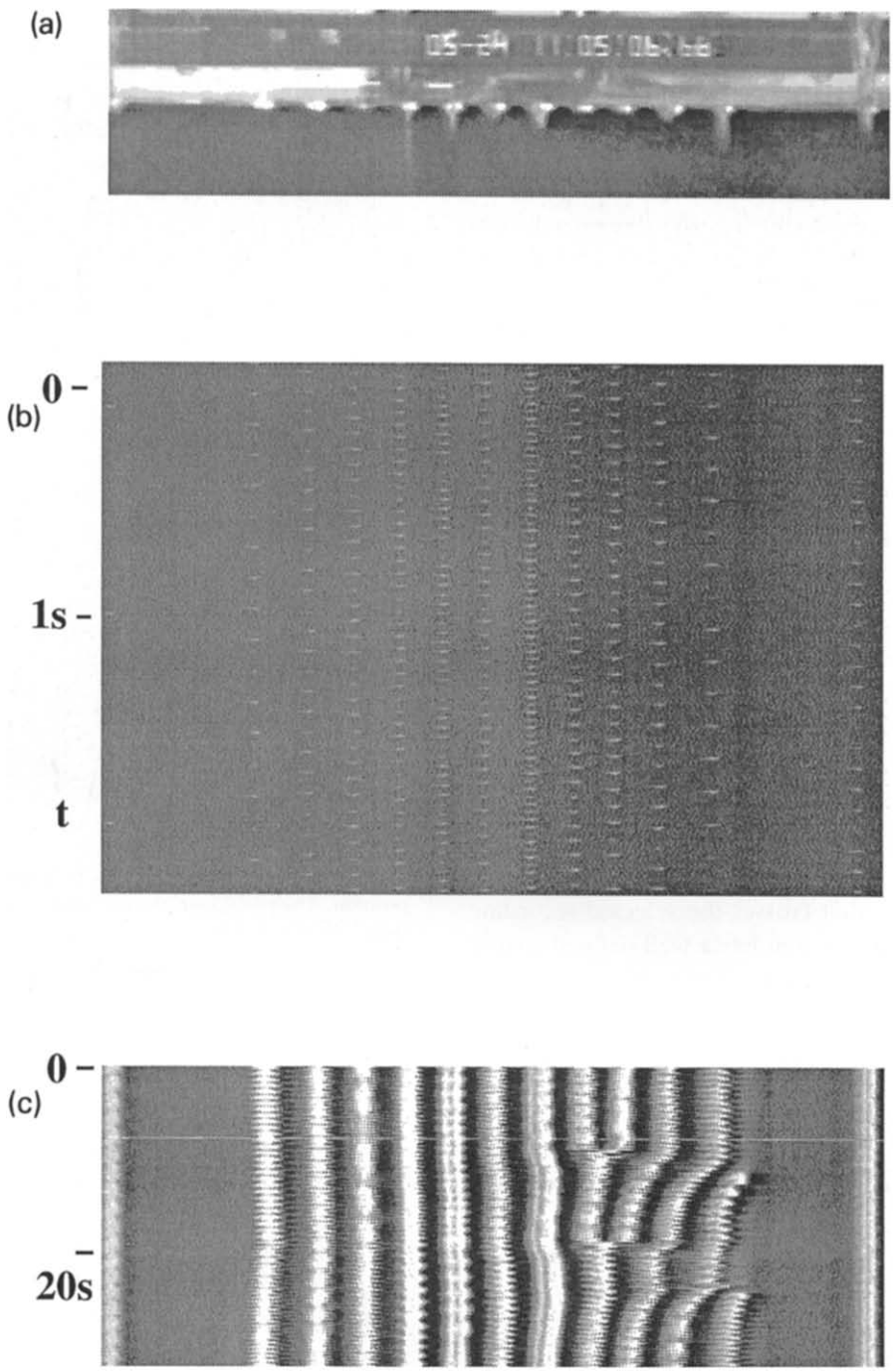

Fig. 8. (a) Dripping regime, and (b), (c) typical spatio-temporal diagrams obtained in this regime. The time runs towards the bottom. Each white spot represents a drop emission (field width 23 cm, viscosity $\eta = 22$ cP, flow rate $Q = 0.9\ \mathrm{cm}^3/\mathrm{s}$).

discuss later. The mean spacing is independent of Q (and of the viscosity), and practically equal to the "capillary" wavelength obtained in the Rayleigh–Taylor instability of a film without continuous supply discussed in section 2. As mentioned above, the wavelength of the structures is locally perturbed by dynamical processes: coalescence of cells, nucleation of new cells, oscillations of the jet position, wave propagation. We have studied these phenomena by using a line of the digitized picture recorded by a video camera, stored at constant time intervals. The line is of course horizontal, and is in general selected as close as possible to the bottom of the cylinder. This avoids possible problems of delays in the position of the jets, when these ones are travelling. The resulting spatio-temporal diagrams are shown in figs. 8–12.

3.2. *Dripping regime*

Fig. 8 shows a diagram obtained in the dripping regime. The spatial coordinate x corresponds to the horizontal axis, while the time runs downwards. Each white spot corresponds to the fall of a drop, that crosses the selected recording line. This phenomenon has a well defined spatial and temporal periodicity. The frequency of drop emission is clearly not uniform in space, a fact probably related to the imperfections of the cylinder, that has been found to be slightly curved under the weight of liquid. At larger time scales (see the same figure), coalescence phenomena appear near the center, that are compensated by nucleations of new cells at the boundaries. It is interesting to note that the pairing of two sites induces a travelling perturbation of the position of the other sites, together with a damping effect. This behavior, reminiscent of problems of phase diffusion [25], suggests that each site is in fact coupled with its nearest neighbors. This effect does not seem however to couple the frequencies of drop emission for the selected values of the flow rate.

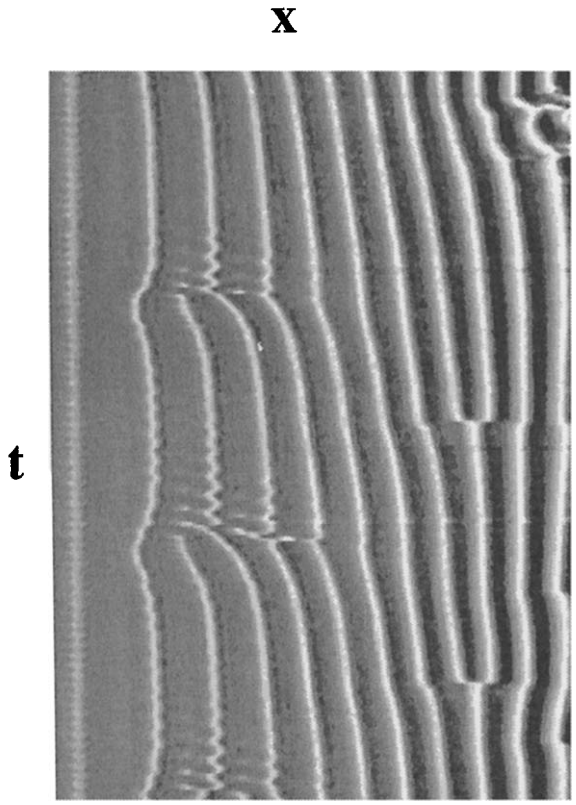

Fig. 9. Spatio-temporal diagram obtained in the "jet" regime. The white lines indicate the evolution of the jet position. The position of the first structure at the left (site of drop emission) has been forced during the experiment ("hard" boundary conditions). The isolated white dots represent a transient pending drop formed between two oscillating jets (see also fig. 10). The picture covers 9.4 cm × 23 s (η = 2 cP, $Q = 7\ \mathrm{cm}^3/\mathrm{s}$).

3.3. *Jet regime: sources, sinks, oscillations*

Pairing and nucleation phenomena similar to those observed in the dripping regime are also obtained in the jet regime. An example is reproduced in fig. 9, where the white lines indicate the position of the jets. We believe that these effects

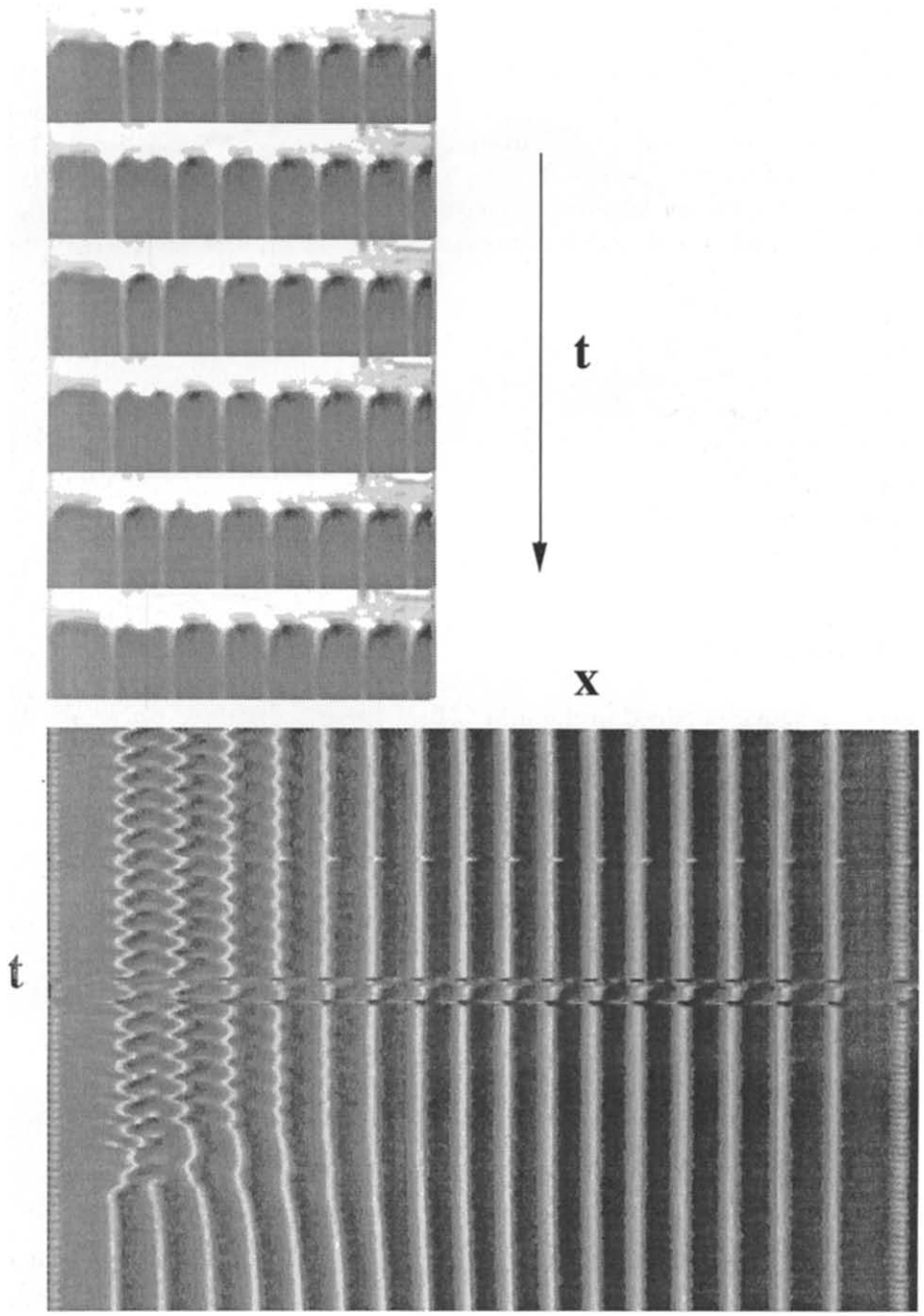

Fig. 10. Oscillations of the jets observed in the "jet" regime (23 cm × 11 s, $\eta = 22$ cP, $Q = 8\ \mathrm{cm}^3/\mathrm{s}$). This oscillation disappears when a new cell is formed.

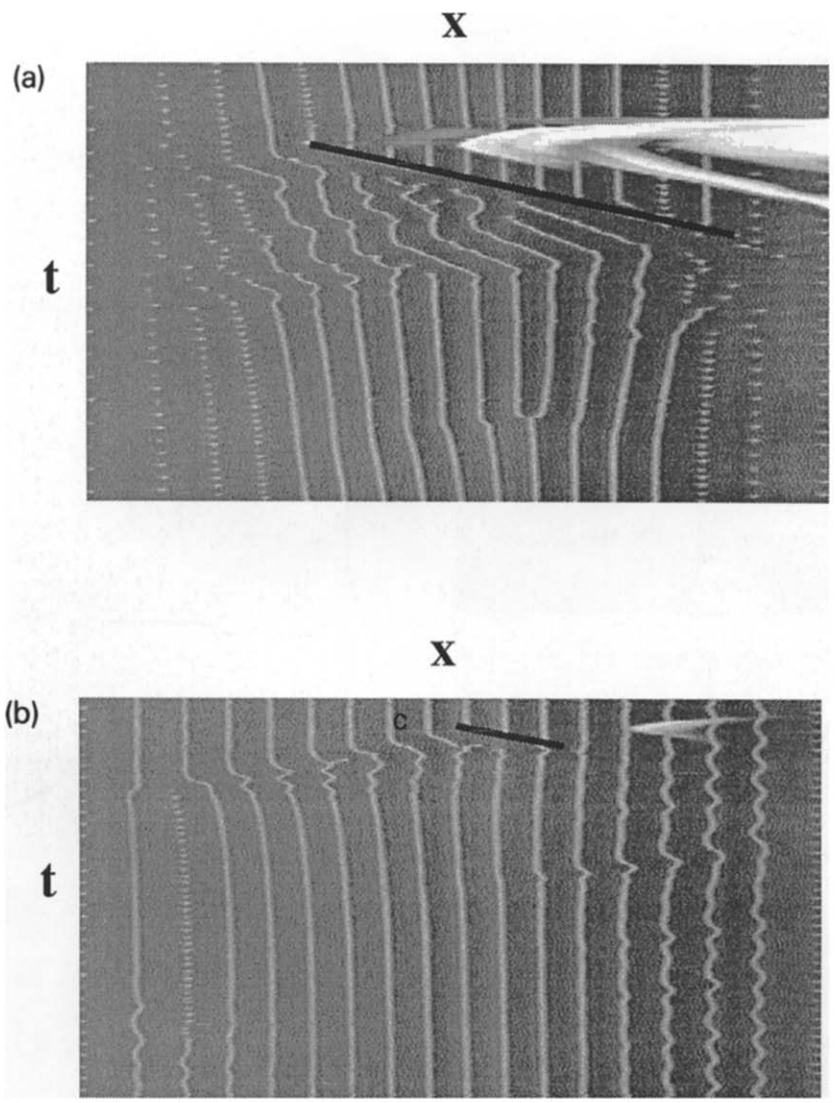

Fig. 11. Two examples of forced "tilt waves" obtained by displacing a needle along the interface ((a) 23 cm × 9.5 s and (b) 23 cm × 9 s, $\eta = 22$ cP, $Q = 3.5\,\mathrm{cm}^3/\mathrm{s}$). The trajectory of the needle is suggested by a black line.

are also due to the slight bending of the cylinder under the weight of liquid, the central part being slightly depressed.

The main difference with the dripping regime is the occurrence of local oscillations of the jet position just before the nucleation takes place. Another example of such oscillations is given in fig. 10. The oscillation of two neighboring jets is associated to the transient formation of a pendant drop appearing and disappearing one time during each period. This drop is also visible (isolated white spots) on the spatio temporal

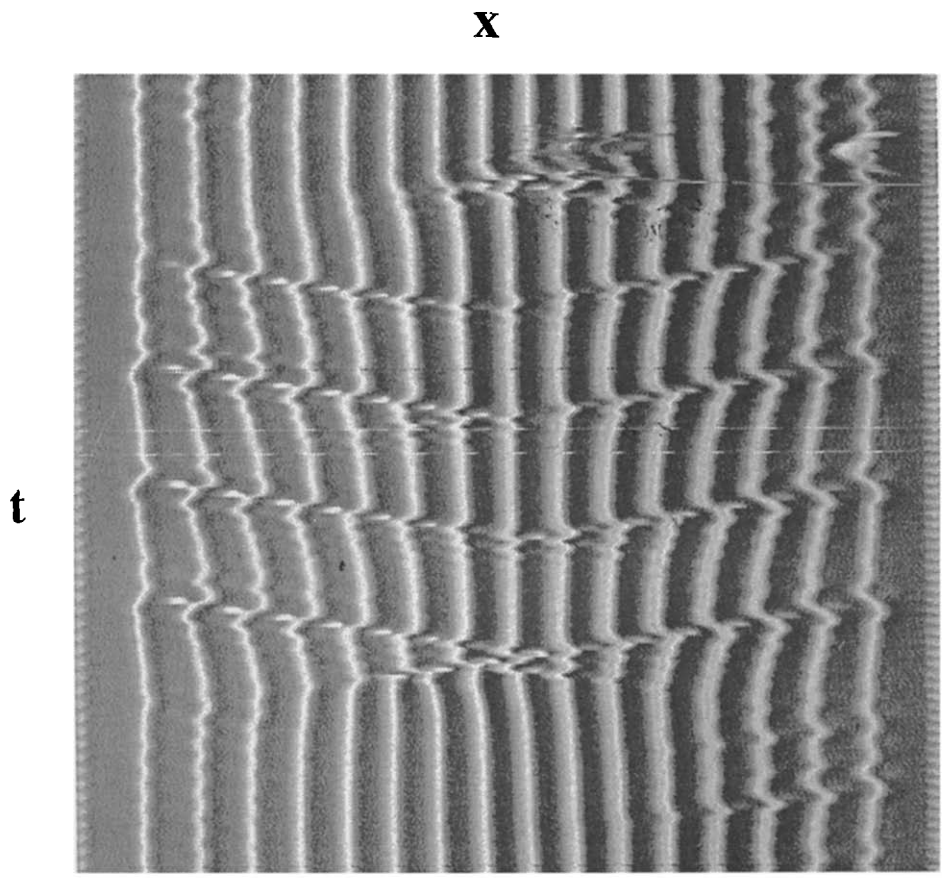

Fig. 12. Spatio-temporal behavior observed after forcing the coalescence of two jets in the central region (23 cm × 16 s, $\eta = 22$ cP, $Q = 5.5\ \mathrm{cm}^3/\mathrm{s}$).

diagram of fig. 9. The oscillation disappearing after the nucleation of a new cell, we suggest that it may come from a phase instability associated to a locally too large value of the wavelength. This too large value could be due to the tendency of the jet to drift towards the central region, combined with the "hard" boundary conditions that we have imposed: the positions of the two extreme jets has been forced by roping two thin wires on the cylinder. Such oscillations are also reminiscent of those observed in the printer instability [16], in the vicinity of abnormal cells.

3.4. *Jet regime: forced tilt waves*

An interesting feature of our system is the possibility to force the positions of the jets and dripping sites. This can be achieved very easily by touching the jets or the pendant drops with a needle, and by moving the needle. When this motion takes place at a large enough speed, a coherent drift of a group of cells can be initiated. This gives rise to "tilt waves" analogous to those observed in other one-dimensional systems [16–19]. Two examples are depicted in fig. 11, respectively associated to a phase shift of nearly 4π

and 2π. After a rather short propagation, the tilt waves are eliminated by nucleation of new cells. In the second example, jet oscillations accompany the tilt wave. This effect is similar to that pointed out recently by Michalland and Rabaud [26] for the printer instability and may reveal an "elasticity" of the jet pattern.

Finally, in fig. 12 we present a behavior forced by a slightly different method: we have touched the bottom of the cylinder with a needle just between two jets located near the center of the sample. This has forced the coalescence of the two jets. Just after the coalescence, two dilatation waves propagate towards the boundaries. This step is followed by an increase of the jet oscillations near the boundaries, coupled with periodic emissions of damped "tilt waves" towards the center. These "tilt waves" involve a transient pendant drop similar to that observed in the oscillation phenomena (see section 3.3). Finally, the initial periodicity has been recovered by nucleation of a new cell.

4. Conclusion

The results given by the recent experiments presented in this article can be summarized as follows:

(1) The two-dimensional structure formation in liquid films submitted to a destabilizing gravity observed in our previous studies seems to arise by processes of front propagations. These fronts separate two states (unperturbed interface–rolls, rolls–hexagons, unperturbed interface–annuli) the first one being unstable compared to the second one.

(2) At the accuracy of our measurements, the properties of the simplest kind of front (formation of rolls) are well described by the theory of linear marginal stability. However, the structure of the evolution equation of the interface suggests that non-linear marginal stability may hold. Numerical studies of this problem are underway [27,28].

(3) When the unstable film is continuously supplied with liquid, this transient structure formation phenomenon can be followed by a "steady" state that we have studied in a one-dimensional situation. At low flow rate one obtains a periodic array of sites of drop emissions ("dripping regime"), the drop emission being also periodic in time. At intermediate flow rate, a periodic array of jets (or columns) is formed the elimination of liquid becoming continuous in time ("jet regime"). At large flow rate, the array of jets is replaced by liquid sheets.

(4) The spatial periodicity of the jets and drops arrays does not seem to depend (or at least is only weakly dependent) upon the flow rate, and seems to coincide with that observed without an external source of liquid (wavelength of the Rayleigh–Taylor instability of thin films, close to $\lambda_M = 2\pi\sqrt{2}\, l_c$, $l_c = \sqrt{\gamma/\rho g}$ being the capillary length). This spatial periodicity is however locally perturbed by phenomena similar to those observed in other one-dimensional systems: oscillations, pairing, tip-splitting, tilt waves.

More accurate studies of the problems of front propagation are under way in the two-dimensional case without external source. This system is interesting for the following reasons:

(1) Two-dimensional effects can be observed (annular patterns, inclined fronts, fronts separating different symmetries), and very few results are known in this case. Numerical results are available [12] but remain to be tested.

(2) As mentioned in section 2.3, the linear part of the evolution equation is close to that of the Swift–Hohenberg equation, but with a control parameter forced to the value $\varepsilon = 1$. This means that we are in fact in a situation far from any threshold and the usual approximations (separation of scales, amplitude equations) cannot be made. To our knowledge, marginal stability has never been tested experimentally under such conditions.

(3) Although we did not present here experiments of this kind, patterns of different symmetry orders can be forced very easily by external perturbations (arrays of needles for instance). This allows us to study very easily the stability of each pattern and its possible destabilizing mechanisms.

Experiments on films under continuous supply are also under way. Again, the possibility to force position of the cells by simply touching the interface, allows to study very easily the phase dynamics in this stability. We also plan to study the two-dimensional case, the injection of fluid taking place across a porous medium.

Acknowledgement

Our understanding of problems of front propagations, has benefitted from discussions with H. Brand, W. Van Saarloos, G. Dewell and D. Walgraef. We acknowledge helpful discussions with P. Bergé, O. Cardoso, Y. Couder, G. Faivre, P. Kurowski, S. Michalland, C. Misbah, M. Rabaud, P. Tabding, R. Thomé and H. Willaime about the behaviors observed in their one-dimensional systems. We thank C. Allain, M. Cloitre and J.M. di Meglio for having measured very accurately the physical properties of the used oils. We also thank A. Fardika of Stone Age Society, for software improvement in image processing.

References

[1] T.P. Hynes, Stability of thin films, Ph.D. Thesis, Cambridge University (1978).
[2] A.J. Babchin, A.L. Frenkel, B.G. Levich and G.I. Sivashinsky, Phys. Fluids 26 (1983) 3159.
[3] S.G. Yiantsios and B.G. Higgins, Phys. Fluids A 1 (1989) 1484.
[4] M. Fermigier, L. Limat, J.E. Wesfreid, P. Boudinet, M. Petitjean, C. Quilliet and T. Valet, Phys. Fluids A 2 (1990) 1517.
[5] M. Fermigier, L. Limat, J.E. Wesfreid, P. Boudinet and C. Quilliet, J. Fluid Mech. 236 (1992) 349.
[6] J.M. Chicheportiche and J.P. Renaudeaux, communication to the 10th French Congress of Mechanics, 2–6 September 1991.
[7] J. Berenson, Int. J. Heat Mass Transfer 5 (1962) 985.
[8] M. Fermigier, L. Limat, J.E. Wesfreid, P. Boudinet, C. Ghidaglia and C. Quilliet, in: Non-linear phenomena related to growth and form, eds. M. Ben Amar, P. Pelce and P. Tabeling (Plenum, New York, 1991).
[9] G. Dee and J.S. Langer, Phys. Rev. Lett. 50 (1983) 383.
[10] E. Ben Jacob, H.R. Brand, G. Dee, L. Kramer and J.S. Langer, Physica D 14 (1985) 348.
[11] W. Van Saarloos, Phys. Rev. Lett. 58 (1987) 2571; Phys. Rev. A 37 (1988) 211; 39 (1989) 6367.
[12] C. Schiller, Modelisation of microstructures in metals, Thesis, Université Libre de Bruxelles (1989).
[13] R.A. Fisher, Ann. Eugenics 7 (1937) 355;
A. Kolmogorov, I. Petrovsky and N. Piskunov, Bull. Univ. Moscou Ser. Int. Sec. A 1 (1937) 1.
[14] G. Ahlers and D.S. Cannel, Phys. Rev. Lett. 50 (1983) 1583;
J. Fineberg and V. Steinberg, Phys. Rev. Lett. 58 (1987) 1332.
[15] P. Fife, in: Mathematical aspects of reacting and diffusing systems, ed. S. Levin, Lecture notes in Biomathematics, Vol. 28 (Springer, Berlin, 1979);
J. Boissonade, Q. Ouyang, A. Arneodo, J. Elezgaray, J.C. Roux and P. De Kepper, in: Nonlinear waves in processes in excitable media, eds. A.V. Holden, M. Markus and H.G. Othmer (Plenum, New York, 1991).
[16] M. Rabaud, S. Michalland and Y. Couder, Phys. Rev. Lett. 64 (1990) 184.
[17] F. Daviaud, M. Dubois and P. Bergé, Europhys. Lett. 9 (1989) 441;
F. Daviaud, M. Bonetti and M. Dubois, Phys. Rev. A 42 (1990) 3388;
F. Daviaud, J. Lega, P. Bergé, P. Coullet and M. Dubois, to appear in Physica D.
[18] G. Faivre, S. de Cheveigné, C. Guthman and P. Kurowski, Europhys. Lett. 9 (1989) 779.
[19] A. Simon, J. Bechhoefer and A. Libchaber, Phys. Rev. Lett. 61 (1988) 2574;
J. Bechhoefer, A. Simon, A. Libchaber and P. Ostwald, Phys. Rev. A 40 (1989) 2042.
[20] I. Mutabazi, J.J. Hegseth, C.D. Andereck and J.E. Wesfreid, Phys. Rev. Lett. 64 (1990) 1729.
[21] W.G. Pritchard, J. Fluid Mech. 165 (1986) 1.
[22] H. Thomé, M. Rabaud and Y. Couder, unpublished.
[23] P.S. Hammond, J. Fluid Mech. 137 (1983) 363;
P.A. Gaugligtz and C.J. Radke, Chem. Eng. Sci. 43 (1988) 1457.
[24] R. Clift, J.R. Grace and M.E. Weber, Bubbles, drops and particles (Academic Press, New York, 1978).
[25] Y. Pomeau and P. Manneville, J. Phys. (Paris) Lett. 40 (1979) L609;

J.E. Wesfreid and V. Croquette, Phys. Rev. Lett. 45 (1980) 634; M. Wu and C. Andereck, Phys. Rev. A, 43 (1991) 2074.
[26] S. Michalland and M. Rabaud, to appear in this volume.
[27] C. Mitescu, L. Limat and J.E. Wesfreid, Bull. Am. Soc. 35 (1990) 2277. A more detailed report will be published elsewhere.
[28] A. Jiminez-Laguna, unpublished.